Supporting Information

Delemotte et al. 10.1073/pnas.1416959112

SI Materials and Methods

VSD Models Generation. The crystal structure of the Kv1.2 channel was solved in the activated–open state (1) and a refined structure was proposed by Chen et al. in 2010 (2). To produce models of other states of the Kv1.2 VSD, we used a procedure similar to the one described in Wood et al. (2012) (3). Building alignments in which the S4 stretch is shifted by three residues (corresponding to one helical turn) toward the N terminus produced a homology model of a first intermediate state downward of α, which we call β, using the nomenclature proposed in previous work (4, 5). The alignments in which S4 is manually shifted by 6, 9, and 12 residues relative to the original alignment produced states closer to the resting state, called γ, δ, and ε. Note that this procedure results in states that are more stable than the steered MD procedure devised by our group earlier (5, 6).

System preparation. The δ- and ε-state models of the VSD of Kv1.2 [residues 163 (S1) to 324 (S4–S5 linker)] were then inserted in a fully hydrated 110 × 110-Å^2 1-palmitoyl-2-oleoyl-sn-glycero-3-phosphocholine bilayer oriented in the x–y plane using the VMD membrane builder. Overlapping lipids and water molecules were then deleted. The system was then ionized in 0.15 M NaCl. The total number of atoms in the system is ∼100,000.

Molecular Dynamic Simulations. The systems were equilibrated under normal constant temperature and pressure conditions (298 K, 1 atm) in a 150 mM NaCl solution. The lipid tails were melted during the first nanosecond, restraining the position of the protein, lipid head groups, water molecules, and ions to their initial position with a strong harmonic potential. To ensure correct reorganization of the lipids and solution, the positions of all of the atoms of the channel were then restrained for 2 ns. The side chains were then allowed to reorganize while the backbone was kept restrained for 8 ns. Lastly, a 100-ns unrestrained MD simulation was conducted, enabling the system to relax. The MD simulations were carried out using the GROMACS 4.6.5 program (7) using a 2.0-fs time step. Bond lengths were constrained with the LINCS algorithm (8) and SETTLE was used for water molecules (9). Long-range electrostatic forces were taken into account using the particle mesh Ewald approach (10). A 1.2-nm cutoff was used for electrostatic and van der Waals interactions, with a switching function starting at 0.8 nm. Simulations were performed at 300 K by using a Nosé–Hoover thermostat (11). Semiisotropic pressure control was achieved by the Parrinello–Rahman barostat (12). The water molecules were described using the TIP3P model (13). The simulation used the CHARMM22-CMAP force field with torsional cross-terms for the protein (14) and CHARMM36 for the phospholipids (15).

Considerations on the Choice of the Collective Variables. A "good" collective variable enables crossing the free-energy barrier in a reasonable amount of simulation time and leads to convergence of the free-energy surface. Clearly these properties can be only verified a posteriori, thus the choice of collective variables proceeds, in general, through a trial and error process.

Our first attempt has been to use the so-called path collective variables (16). In this approach two collective variables are used to describe a reaction pathway in a high dimensional space: the distance along the pathway and the distance from the pathway. Because several distinct distances can be defined in the configurational space, we tried one based on the rmsd and another one based on contact maps. What turned out to be problematic with these collective variables was their degree of "degeneracy," i.e., the fact that a given value of the collective variable corresponds to a heterogeneous set of microscopic configurations. When this heterogeneity is too large, then equilibrium among these microscopic configurations is never achieved. In this scenario, applying a biasing potential to modify the current value of the collective variable might not be an effective strategy to improve sampling. In practice, forcing a change in the value of the collective variable results in the system relaxing along the "soft" degrees of freedom without ever exploring the "hard" ones. Based on these considerations, we decided not to use the gating charge to bias the dynamics, even though this specific collective variable was never tested.

It is also instructive to comment on the empirical tuning of the k parameter for the CV_{R1} and CV_{R3} collective variables used in this work. For too-small values of k, the biasing potential did not promote crossing of the VSD hydrophobic barrier by R1. Rather, this gating charge dwells for a long time in one of the two binding sites before any jump occurs.

Gating Charge Expression. The gating charge Q can be linked to the microscopic state of the channel through

$$Q = \frac{\Delta G(\lambda_2, V) - \Delta G(\lambda_1, V)}{V},$$

where V is the transmembrane (TM) potential. For each channel conformation (λ), $\Delta G(\lambda,V)$ is the reversible work component due to the applied voltage V. It relates the conformation of the channel to $\delta(\boldsymbol{r}_i^{\lambda})$, the so-called "electrical distance" (17):

$$\Delta G(\lambda, V) = G(\lambda, V) - G(\lambda, 0) = \Delta V \cdot \sum_i q_i \cdot \delta(\boldsymbol{r}_i^{\lambda}),$$

where $\lambda \equiv \{\ldots r_N\}$ is the set of N atomic coordinates of the protein in a conformation λ, q_i is the ith protein charge, and $\delta(\boldsymbol{r}_i^{\lambda})$ is the electrical distance, given by

$$\delta(\boldsymbol{r}) = \frac{\partial}{\partial V}\Phi(\boldsymbol{r}).$$

This quantity accounts for the degree of coupling between the local-electrostatic potential at the position of charge q_i, the electrostatic potential $\Phi(\boldsymbol{r})$, and the TM applied potential V.

In practice, $\delta(\boldsymbol{r}_i^{\lambda})$ is evaluated for each protein configuration λ by carrying out two independent simulations of the system under two different TM potentials V (4). For each V, the local-electrostatic potential $\Phi(\boldsymbol{r})$ is then calculated as an average over $n = 100$ configurations sampled along 2 ns of simulation. For a given conformation λ, the electrical distances were estimated with $\delta \equiv [\varphi^{\lambda}(\mathbf{r},\Delta V_2) - \varphi^{\lambda}(\mathbf{r},\Delta V_1)]/(\Delta V_2 - \Delta V_1)$.

Here, $\delta_i^{\lambda}(z)$ is approximated by the best fit of the measured electrical distance in the γ-state by the generalized logistic function (Fig. S2):

$$\delta(z) = \frac{1}{1 + e^{-\alpha(z-\beta)}}, \text{ with } \alpha = 1.80654 \text{ and } \beta = 0.0949.$$

1. Long SB, Campbell EB, Mackinnon R (2005) Crystal structure of a mammalian voltage-dependent Shaker family K+ channel. *Science* 309(5736):897–903.
2. Chen X, Wang Q, Ni F, Ma J (2010) Structure of the full-length Shaker potassium channel Kv1.2 by normal-mode-based X-ray crystallographic refinement. *Proc Natl Acad Sci USA* 107(25):11352–11357.
3. Wood ML, et al. (2012) Water wires in atomistic models of the Hv1 proton channel. *Biochim Biophys Acta* 1818(2):286–293.
4. Treptow W, Tarek M, Klein ML (2009) Initial response of the potassium channel voltage sensor to a transmembrane potential. *J Am Chem Soc* 131(6):2107–2109.
5. Delemotte L, Tarek M, Klein ML, Amaral C, Treptow W (2011) Intermediate states of the Kv1.2 voltage sensor from atomistic molecular dynamics simulations. *Proc Natl Acad Sci USA* 108(15):6109–6114.
6. Gosselin-Badaroudine P, Delemotte L, Moreau A, Klein ML, Chahine M (2012) Gating pore currents and the resting state of Nav1.4 voltage sensor domains. *Proc Natl Acad Sci USA* 109(47):19250–19255.
7. Hess B, Kutzner C, van der Spoel D, Lindahl E (2008) GROMACS 4: Algorithms for highly efficient, load-balanced, and scalable molecular simulation. *J Comp Theor Chem* 4:435–447.
8. Hess B, Bekker H, Berendsen HJC, Fraaije JGEM (1997) LINCS: A linear constraint solver for molecular simulations. *J Comput Chem* 18(12):1463–1472.
9. Miyamoto S, Kollman PA (1992) Settle: An analytical version of the SHAKE and RATTLE algorithm for rigid water models. *J Comput Chem* 13(8):952–962.
10. Darden T, York D, Pedersen L (1993) Particle mesh Ewald - an Nlog(N) method for Ewald sums in large systems. *J Chem Phys* 98(12):10089–10092.
11. Nosé S (1984) A unified formulation of the constant temperature molecular dynamics methods. *J Chem Phys* 81(1):511–519.
12. Parrinello M, Rahman A (1981) Polymorphic transitions in single crystals: A new molecular dynamics method. *J Appl Phys* 52(12):7182–7190.
13. Jorgensen WL, Chandrasekhar J, Madura JD, Impey RW, Klein ML (1983) Comparison of simple potential functions for simulating liquid water. *J Chem Phys* 79(2):926–935.
14. MacKerell AD, Jr, Feig M, Brooks CL, III (2004) Improved treatment of the protein backbone in empirical force fields. *J Am Chem Soc* 126(3):698–699.
15. Klauda JB, et al. (2010) Update of the CHARMM all-atom additive force field for lipids: Validation on six lipid types. *J Phys Chem B* 114(23):7830–7843.
16. Branduardi D, Gervasio FL, Parrinello M (2007) From A to B in free energy space. *J Chem Phys* 126(5):054103.
17. Sigworth FJ (1994) Voltage gating of ion channels. *Q Rev Biophys* 27(1):1–40.

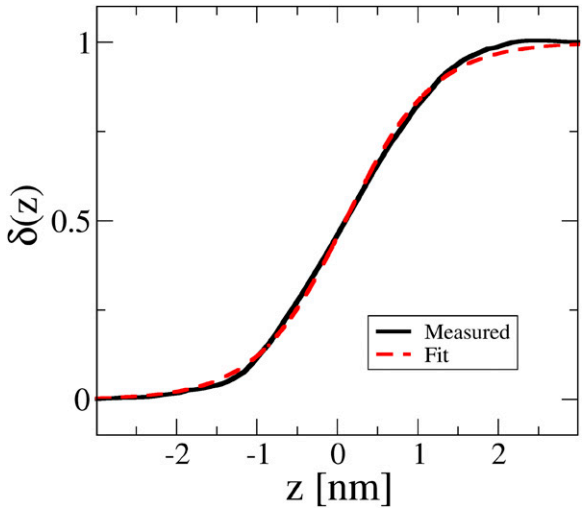

Fig. S1. Electrical distance along the VSD main axis computed as $\delta \equiv [\varphi^{\lambda}(\mathbf{r},\Delta V_2) - \varphi^{\lambda}(\mathbf{r},\Delta V_1)]/(\Delta V_2 - \Delta V_1)$. The best fit by the generalized logistic function is shown in dashed red.

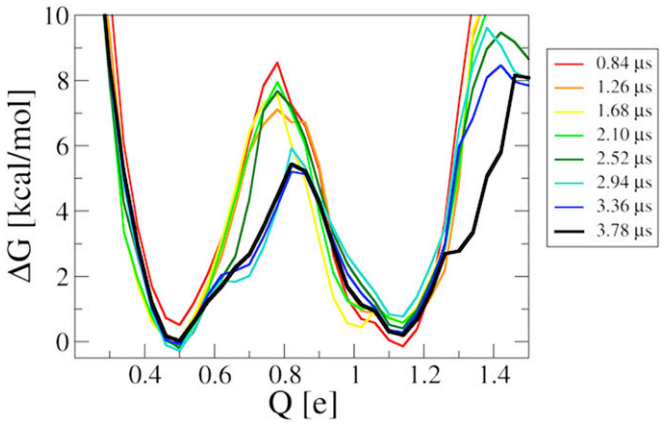

Fig. S2. Evolution of the reweighted free-energy profile as a function of the gating charge *Q* collective variable along the simulation time.

Table S1. Parameters of the switching and fitting functions used to describe the contacts between pairs of residues

Salt bridge partners	d_0, nm	r_0, nm	a	b	c
$R/K - PO_4^-$	0.445	0.041	0.51	6.95	0.32
R-E/D	0.395	0.018	0.46	7.78	0.82

The parameters for the switching functions d_0 and r_0 were determined to fit the equilibrium distribution of distances between pairs of salt bridge partners. The fitting function is used to describe the binding in a quasi-binary fashion (a group is either bound or unbound irrespective of the number of binding partners). a, b, and c are the parameters of a generalized logistic function and ensure that the distance at half-binding matches the one of the equilibrium distribution.